

Spatial Statistics of Spectrum Usage: From Measurements to Spectrum Models

Matthias Wellens, Janne Riihijärvi, Martin Gordziel and Petri Mähönen
Department of Wireless Networks, RWTH Aachen University
Kackertstrasse 9, D-52072 Aachen, Germany
Email: {mwe, jar, mgo, pma}@mobnets.rwth-aachen.de

Abstract—Several measurement studies have found a large amount of underutilized radio spectrum. More flexible regulation employing dynamic spectrum access (DSA) has been proposed as solution to this problem. The analysis of several aspects of DSA systems, e.g., cooperative sensing, requires good spatial models of spectrum usage. However, only very focused models such as propagation or shadowing correlation models exist. In this paper we apply techniques developed by the spatial statistics community to the modelling of spectrum. In more detail, we use random fields and the semivariogram to describe the spatial correlation of spectrum usage. We extract parameters from extensive real-life measurements for multiple wireless technologies. These parameter sets enable other researchers to use the model for different tasks ranging from theoretical to simulation-based studies.

I. INTRODUCTION

Recently, extensive measurement studies have shown that several spectrum bands are underutilized in spatial as well as time domain [1], [2]. A more flexible approach to spectrum regulation enabling Dynamic Spectrum Access (DSA) has been proposed in order to exploit the unused spectral resources [3]–[5]. In the DSA vision, secondary users will be allowed to access vacant spectrum bands in an opportunistic fashion if they strictly limit harmful interference to any licensed primary system. In this context, the task of identifying vacant spectrum, usually called spectrum sensing, is crucial for efficient system operation. Due to signal fading and shadowing effects single secondary users may miss primary transmissions and falsely classify the spectrum band under test as available for opportunistic access. It has been shown that cooperative spectrum sensing is one possible solution to this problem [6]–[8]. Based on models for correlation of shadowing experienced by nearby users, see e.g. [9], it has been further shown that correlated shadowing lowers the cooperation gain. Although these models have been very useful, their applicability is limited due to the focus on cellular networks and the lack of two-dimensional extensions.

In this paper we apply techniques from spatial statistics to the modelling of spectrum. We introduce the semivariogram as flexible model and discuss its application to DSA research. Semivariogram-based modelling has also been applied in sensor networks research to model spatially correlated phenomena [10]. In the case of DSA the power spectral density (PSD) measured in a certain spectrum band is one of the key values to be modelled. We provide complete parameter sets for PSD models based on different wireless technologies in

order to enable other researchers to easily use the proposed spectrum model. All given parameters have been extracted from extensive real-world spectrum measurements. The work discussed in this paper is an extension of the early results presented in [11].

Stochastic models for the spectrum and especially for the PSD have many potential applications. The most obvious of these is the creation of realistic models for simulation purposes. Comprehensive evaluation of protocols and algorithms for, e.g., DSA networks requires proper models, which have not been available so far. Our results can be seen as a first step towards the development of such tools. We also expect that the developed PSD correlation models can be used in analytical calculations to, for example, further refine results on collaboration gain in spectrum sensing.

Finally, correlation structures can be used to improve prediction of spectrum usage at regions enclosed by measurement locations but for which measurements are not directly available. Such prediction techniques could be used in, for example, the future cognitive wireless networks. The nodes in such networks will optimize the network configuration, e.g., the details of the cooperative sensing scheme, in an online fashion. The underlying reasoning requires comprehensive models for the environment and the approaches presented in this paper are good candidates for the representation of several characteristics of the radio environment.

The rest of this paper is structured as follows. In Section II we introduce the basic modelling approach. After commenting on our measurement setup in Section III, we present results for different wireless technologies in Section IV. We conclude the paper in Section V.

II. SPATIAL STATISTICS

The methods, that we apply in this paper, have been developed in the context of geostatistics, which is seen as a subfield of spatial statistics [12]. These models, that describe certain properties of soil, are needed in numerous applications such as mining, geology, or agriculture. Since sampling the soil is an expensive task and variation in soil is complex, the sufficient description of a soil property by a deterministic model is unrealistic. Instead, geostatistical techniques describe the concentration of ore or other soil properties using statistical models. They treat the examined phenomenon as a realization

of a *random field* $Z(\mathbf{u})$ based on the model

$$Z(\mathbf{u}) = \mu + \epsilon(\mathbf{u}), \quad (1)$$

where μ is the mean¹ and $\epsilon(\mathbf{u})$ is a random residual. We use the capital letter Z in order to show the relationship of multi-dimensional random fields to usual one-dimensional stochastic processes. The location $\mathbf{u} \in D$ lies in the domain of interest D , which is part of \mathbb{R}^2 or \mathbb{R}^3 , depending on the applied model and the sampling setup.

In order to provide complete models based on few samples, geostatisticians enabled the robust prediction of a soil property at an arbitrary position based on its correlation to the soil property measurements taken at the sampling locations. More in detail, they developed models for the spatial autocorrelation of the above introduced random residual $\epsilon(\mathbf{u})$, which we express with the semivariogram²

$$\begin{aligned} \gamma(\mathbf{u}, \mathbf{v}) &= \frac{1}{2} \mathbb{E}[(Z(\mathbf{u}) - Z(\mathbf{v}))^2] \\ &= \frac{1}{2} \mathbb{E}[(\epsilon(\mathbf{u}) - \epsilon(\mathbf{v}))^2], \text{ with } \mathbf{u}, \mathbf{v} \in D, \end{aligned} \quad (2)$$

where \mathbb{E} signifies expectation.

We can often assume Z to be (second-order) stationary, making γ to depend only on the vector between the two locations $\mathbf{h} \equiv \mathbf{v} - \mathbf{u}$. If Z is also isotropic it will depend only on the distance $h = \|\mathbf{h}\|$. In the case of second-order stationarity the relationship to the equivalent autocovariance function can be written as

$$\begin{aligned} C(\mathbf{h}) &= \mathbb{E}[(Z(\mathbf{u}) - \mu)(Z(\mathbf{u} + \mathbf{h}) - \mu)] \\ &= C(\mathbf{0}) - \gamma(\mathbf{h}), \end{aligned} \quad (3)$$

where $C(\mathbf{h})$ denotes the autocovariance at lag \mathbf{h} and $C(\mathbf{0})$, the autocovariance at lag zero, is the variance of the process. We further define the spatial *correlogram* $\rho(\mathbf{h}) = C(\mathbf{h})/C(\mathbf{0})$, the spatial analog of the autocorrelation function, which in the literature is also referred to as correlation function.

Finally, we rewrite the semivariogram to end with a more descriptive representation:

$$\gamma(\mathbf{h}) = \tau^2 + \sigma^2(1 - \rho_0(\mathbf{h}/\phi)), \text{ with } \tau^2 \in \mathbb{R}_0^+, \sigma^2, \phi \in \mathbb{R}^+, \quad (4)$$

where τ^2 is the sampling error, which usually should be zero. It is also called the *nugget variance* because in mining sampling errors can occur due to the rare occasion of single nuggets of ore. The variance of the process $C(\mathbf{0}) = \sigma^2$ is also called the *sill* because $\lim_{\tau^2=0, \|\mathbf{h}\| \rightarrow \infty} \gamma(\mathbf{h}) = \sigma^2$. The parameter ϕ , defined via $\rho(\mathbf{h}) = \rho_0(\mathbf{h}/\phi)$, controls the *range* of the model, meaning at which distance no correlation³ is

¹In more complex models the mean is location-dependent because of present trends in the data but we limit the discussion to the simplest form in order to focus on the underlying concepts.

²In literature the semivariogram is often denoted simply by variogram although the latter term refers to the definition without the coefficient 1/2.

³For asymptotically silled semivariograms, two points will only be spatially uncorrelated in the limit as $\|\mathbf{h}\| \rightarrow \infty$. In this case, we speak of the *effective range*, which is not uniquely defined [13] but roughly corresponds to 95% of the sill. Additionally, there exist semivariogram models that are not asymptotically silled but we do not take those into account here because the modelled processes are non-stationary.

anymore present, i.e. $\rho_0(\mathbf{h}/\phi) = 0$.

A. Model generation

An artificial model is sufficiently described by the selected type of correlation function ρ_0 and all required parameters including the average value μ . Several techniques have been proposed to determine appropriate parameter sets. Most notably there are the maximum likelihood estimation [14], further extensions towards Bayesian inference [13], and the least squares based estimation [12], [15]. Here, we focus on the latter approach because of its wide spread in geostatistical literature. We apply weighted least squares estimation (WLSE) because of its good tradeoff between performance and complexity [12], [15].

The complete process of model generation consists of the following three steps:

First, we require an estimate of the semivariogram computed from the available samples. We selected the *empirical semivariogram* by Matheron [16], which is the most popular one in literature. Other estimators are presented in [12] and [15]. The algorithm applies binning to group sample-pairs at similar distances. In this context, let $N(h)$ denote the set of pairs (i, j) such that $h - \Delta \leq \|\mathbf{x}_j - \mathbf{x}_i\| < h + \Delta$, where $\mathbf{x}_i, \mathbf{x}_j \in D$ and $\Delta \in \mathbb{R}^+$. Averaging over all sample-pairs in each bin then yields

$$\hat{\gamma}(h) \equiv \frac{1}{2|N(h)|} \sum_{N(h)} (Z_j - Z_i)^2. \quad (5)$$

Second, we have to choose an appropriate model for the semivariogram γ before we can start the parameter estimation. Adapted to the above form for the semivariogram given in (4), popular functions used in geostatistics are the *exponential model*

$$\gamma_{\text{exp}}(h) = \tau^2 + \sigma^2(1 - \exp(-h/\phi)), \quad (6)$$

the *Gaussian model*

$$\gamma_{\text{G}}(h) = \tau^2 + \sigma^2[1 - \exp(-(h/\phi)^2)], \quad (7)$$

and the very general *Matérn model*

$$\gamma_{\text{M}}(h) = \tau^2 + \sigma^2 \left(1 - \frac{1}{2^{\kappa-1}\Gamma(\kappa)} \left(\frac{h}{\phi} \right)^{\kappa} K_{\kappa} \left(\frac{h}{\phi} \right) \right), \quad (8)$$

where $\kappa \geq 0$ is a fourth model parameter, Γ is the gamma-function, and K_{κ} is the modified Bessel function of the second kind. The Matérn model gives the exponential and Gaussian models as the special cases $\kappa = 1/2$ and $\kappa \rightarrow \infty$, respectively. Additionally, we consider the *Cauchy model*

$$\gamma_{\text{Cau}}(h) = \tau^2 + \sigma^2 \left[1 - (1 + (h/\phi)^2)^{-\kappa} \right], \text{ with } \kappa \geq 0, \quad (9)$$

as one example for models with power-law characteristics.

In geostatistics often further polynomial models, such as the spherical, the cubic, or the penta model, are also considered but those did not provide significantly different results for our source data. The interested reader is referred to [14] or the documentation of the `geoR` package [17] and the `RandomFields` package [18] for the R environment [19] for further details.

Third, we apply the WLSE in order to fit the model γ_{model} , which we selected in step two, to the empirical semivariogram $\hat{\gamma}$, that we estimated in step one.

III. MEASUREMENT SETUP

The power spectral density (PSD) measured over a frequency band of interest is the phenomenon whose spatial statistics we want to capture. We performed distributed spectrum measurements in two scenarios in downtown Aachen, Germany, and at the CeBIT industry fair in Hanover, Germany, in March 2008. The latter is certainly an unusual scenario in terms of wireless service usage but also in this extreme case we found significant amount of spectrum to be unused.

During each of these measurement campaigns we collected PSD samples at all locations of a regular grid and averaged over all samples gathered at the same position. In Aachen we used a grid step size of ≈ 15 m in order to investigate short range services, namely Digital Enhanced Cordless Telecommunications (DECT) and Wireless Local Area Networks (WLAN). For mid-range technologies, such as cellular networks and possibly also the terrestrial version of Digital Video Broadcasting (DVB-T), we used a grid step size of ≈ 250 m. At the CeBIT we measured the WLAN traffic in two connected halls with a grid step size of ≈ 12.5 m.

We moved one measurement setup from grid point to grid point and placed another one statically at a central location in the examined area. The measurement trace of the static setup enables us to verify that the impact of the time of day is rather small and the average PSD results measured by the mobile setup can be used as input for spatial modelling of spectrum.

Both measurement setups use GPS for localization and are based on portable spectrum analyzers and wideband, omnidirectional antennas. Further details are given in [20].

A. Preprocessing of spectrum measurement data

Several wireless technologies transmit non-continuous signals because of underlying time duplexing, frequency hopping, or other techniques. Therefore, our spectrum analyzer based measurement setups might sometimes sweep through a frequency during an ongoing transmission and might sometimes miss it. A similar effect can be caused by systems with low duty cycles (DC)⁴. Since we average over all samples taken at each measurement location, intermediate noise samples will result in a lower average PSD and a usually higher variance of the whole process.

In order to compensate for these unintentional effects we have applied energy detection to the measured samples and have considered only those samples above the detection threshold for averaging and spatial modelling later on. We have used the threshold $\delta = -105$ dBm/100 kHz as reasonable tradeoff between probability of false alarms triggered by strong noise samples and the probability of missed detections of weak

primary signals⁵. We have applied the described threshold only in the case of non-continuous primary transmissions.

Additionally, we have slightly adapted the binning process applied during the estimation of $\hat{\gamma}(h)$ to our sampling grid. Each estimated $\hat{\gamma}(h)$ value is placed exactly at distance h in the middle of the corresponding bin although the distances grouped to this bin may be far from being uniformly distributed over the bin. Instead, we have moved each estimated $\hat{\gamma}(h)$ value from the distance h in the middle of the bin to the distance \bar{h} , the average of all distances in the bin. The more accurate representation of the semivariogram enables a more realistic model fitting later on. Similar enhancements of the sampling and model fitting process are also discussed in [22].

Multiple services are transmitted by spatially distributed primary transmitters, use wideband signals, and are active on more than a single channel. In addition to the averaging over all samples taken at one location, we also average over all PSD samples in one wideband channel. In order to combine different channels we also average over the empirical semivariograms $\hat{\gamma}(\bar{h})$ per channel before we apply the WLSE. For example, in the case of the Universal Mobile Telecommunications System downlink (UMTS DL) we average over all PSD samples taken at one location and in one UMTS DL channel of 5 MHz, compute $\hat{\gamma}(\bar{h})$ for each actively used channel, average over these empirical semivariograms, and finally, estimate model parameters using WLSE.

IV. RESULTS

After we have introduced the underlying model structure and have described our measurements we continue with the results of our modelling work. We will use the very general Matérn model since it provides good results in all cases although the performance of nearly all discussed models is sufficient. Figure 1 shows the fitted semivariograms for three different services including the estimated empirical semivariograms. Since all shown services employ continuous transmissions we have not applied any threshold to the collected measurement data. The further preprocessing techniques have always been applied. In the case of the UMTS DL the estimated curve fits the empirical semivariogram well and also the estimated effective range of about 800 m is realistic for a cellular system. The fitted nugget is very low as we have expected. Both other services, the pager service and DVB-T transmit on significantly lower frequencies and emit higher transmit powers compared to UMTS base stations. Both facts result in a more uniform PSD over space and, thus, a lower sill compared to the UMTS DL.

The sample grid, that we investigated during our measurements, seems to be too small to capture the spatial statistics of the longer range DVB-T and pager services. At the examined distances the range is not reached, yet, causing the model

⁴Let DC describe the fraction of the measurement time during which the examined frequency band is in use by the primary system.

⁵Lower thresholds such as proposed for IEEE 802.22 [21] could not be used due to the narrow resolution bandwidth of 100 kHz and the slightly worse sensitivity of the portable spectrum analyzers. Since our setups needed to run autonomously on batteries highly sophisticated instruments could not be used.

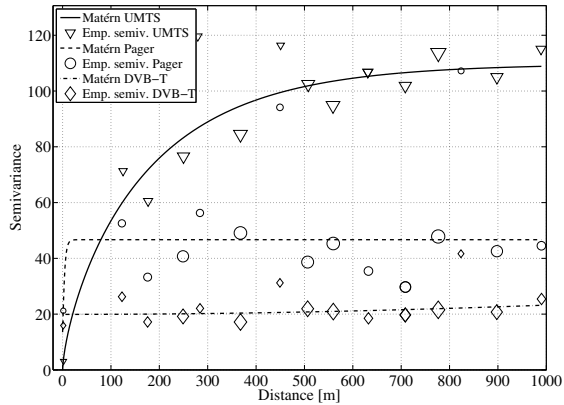


Fig. 1. Fitted semivariograms based on the Matérn-model and estimated empirical semivariograms for the UMTS DL (5 MHz bandwidth per channel, average over five channels at frequencies $f \in [2110, 2170]$ MHz), a pager-service (200 kHz bandwidth at $f = 466$ MHz), and DVB-T (6 MHz bandwidth per channel, average over three channels at $f_1 = 490$ MHz, $f_2 = 498$ MHz, and $f_3 = 514$ MHz).

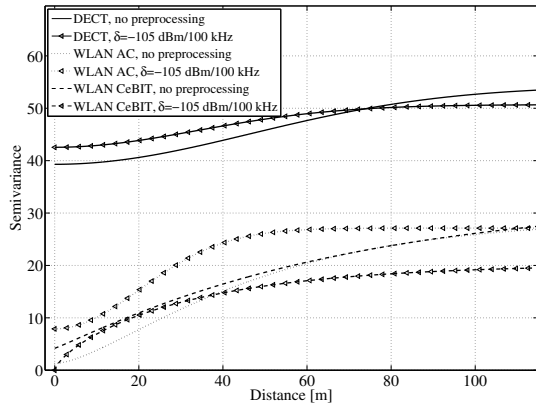


Fig. 2. Fitted semivariograms based on the Matérn-model for the unchanged and the preprocessed input data sets for DECT networks (≈ 1.7 MHz bandwidth per channel, average over ten channels at frequencies $f \in [1880, 1900]$ MHz) and the WLAN system (20 MHz bandwidth per channel, average over the most popular channels 1, 6, and 11 in the 2.4 GHz ISM-band).

fitting to estimate a wrong range of few meters. These examples show that accurate modelling of both services requires either further more distant sampling points or an increased sampling grid step size. However, the selected sampling design is appropriate for the UMTS technology.

Next, we discuss the impact of the threshold application during the data preprocessing. Figure 2 shows two graphs per measurement campaign, namely one for the unprocessed and one for the thresholded data set. We compare the Aachen downtown results for the DECT system to the WLAN case as measured in Aachen and at the CeBIT in Hanover.

At first we focus on the two WLAN measurements. The results show a major dependence of the estimated semivari-

ogram on the DC. At the CeBIT we found a high amount of WLAN usage, see [20] for details. Additionally, nearly all received signals were rather strong because most of the access points (APs) in range were installed inside the exhibition hall. After sorting out the noise samples most of the PSD values are at similarly high values and the variance of the process, represented by the sill, decreases.

The Aachen scenario is more diverse and the propagation environment is more complex due to the numerous buildings. The sill seems to be independent of the preprocessing because two contrary effects compensate each other. On the one hand, the lowest PSD values are sorted out by the threshold application and we expect a lower variance. On the other hand, these very low PSD values were the vast majority and their deletion results in a more uniform distribution of the remaining PSD samples.

In contrast to the sill, the range is clearly different after the threshold application. In Aachen the DC was very low and the dominating noise samples are very similar at all locations indicating high correlation also between further away measurement locations. This wrongly detected correlation is taken out by the application of the threshold δ . Thus, the Aachen results resemble a typical WLAN scenario with little amount of traffic and urban propagation characteristics. The CeBIT data set represents an extreme case with high DCs and an open environment without big obstacles.

For the DECT results the sill is slightly lower for the preprocessed data. The noise samples that are considered in the case without preprocessing are obviously lower than all other samples and increase the variance. The sill and the range are both higher for the DECT system than for the comparable WLAN Aachen case. The higher supported transmit power and lower frequency, that DECT cordless phones use, cause this difference.

The high nugget variance is due to several effects. Basically, we can differentiate two types of effects that can result in a nugget variance. First, every measurement is subject to measurement errors and other location-independent effects. Second, the examined system may have certain characteristics that are location-dependent and change the measurement result. In the use case of wireless communication examples for the former type of noise could be measurement noise of the instrument or primary user power control. Power control will change the received PSD at all locations inside the coverage area independently of the exact location. Examples for the location-dependent factors are shadowing or multipath effects but could also be the number of different active users in an uplink channel.

Before estimating the model parameters we average over multiple samples taken at the same location and adjacent frequency channels that belong to the same wideband signal. Thereby, we lower the impact of the location-independent sources of nugget variance. However, the location-dependent sources will still result in a nugget $\tau^2 > 0$.

Furthermore, the DECT system is another good example for the importance of the sampling grid. Due to the applied regular

sampling grid the number of measurement location pairs at close distances is limited. We performed one measurement with both setups next to each other which is the only result at distances shorter than the grid step size of 15 m. Although the WLSE takes $N(h)$, the number of available location pairs per distance bin, into account during the model fitting, outliers may still result in less probable results. The unexpectedly high nugget for the DECT system is such a case.

During the campaign based on the larger grid we reexamined the DECT system for comparison of the two sampling grids. In the case of the long-range services we have seen that the sampling grid step size of ≈ 250 m is too small to cover the range of these systems. In the case of DECT, this grid step size is too large also causing the model fitting to fail. Further discussion on the selection of an appropriate sampling grid is provided in [22].

A. Model parameters

After we have discussed different cases in more detail we list in Table I the fitted model parameters for the examined wireless technologies. We include parameters for three different model archetypes for the semivariogram. First, the exponential model gives good results and is attractive because three parameters are enough to fully describe it. Second, the Matérn model is a very flexible option because it can mimic both, the Gaussian as well as the exponential model, and has never failed to provide good fits in our tests. Third, the Cauchy model represents a compromise between both cases. It uses four parameters but does not rely on theoretically less tractable terms such as the gamma- or the modified Bessel function. Additionally, it results also in very good fits as can be seen from the quality of fit metric Q . Since our fitting procedure is based on least squares, lower values indicate better fits.

We list parameter sets for both WLAN measurement campaigns for completeness but recommend to use the parameters for the Aachen campaign due to the exceptionality of the CeBIT environment. We did not include the pager and the DVB-T service due to the unreliable sampling. In addition to UMTS we also provide results for another cellular technology, namely the Global System for Mobile Communication (GSM) in its version specified for 900 MHz. Since we performed all our cellular network measurements in the downtown area of Aachen we expect the examined networks to be interference-limited. Therefore, the difference in range between UMTS and GSM900 is smaller than one may expect for large cells. Qualitatively, both cellular technologies show similar characteristics. If applicable we list only the model parameters for the preprocessed data sets.

Although we initially introduced all model parameters with a descriptive meaning not all the given parameter sets do follow this representation. In some cases with higher values for the fourth parameter κ or the nugget variance τ^2 , the range ϕ does not correspond to the distance at which the correlation vanishes. Additionally, all estimated empirical semivariograms are only asymptotically silled and the range parameter does not always fit well to the *effective range*.

The interested researcher may chose the model based on his own requirements and use case. For theoretical studies the exponential and the Cauchy model are certainly interesting. In simulation-based evaluations the added complexity for the Matérn model may be acceptable and its popularity in the spatial statistics community may be another reason for selecting it.

Simulation of random fields can be achieved, e.g., with the `RandomFields` package [18] for the R environment [19]. It supports all the discussed correlogram models and is well documented. Samples of Gaussian random fields with the listed parameters can be generated and used as basis in other simulation frameworks. In addition to the correlogram parameters, Table I also lists the average PSD μ that we computed from our measurement data as follows: First, we compute μ_{ch} , the average PSD over the whole random field per channel of a wireless technology. Afterwards, we also average over those channel-specific values resulting in the listed value $\overline{\mu_{ch}}$. Additionally, let $\text{std}(\mu_{ch})$ denote the standard deviation of those channel specific values.

V. CONCLUSION

In this paper we have proposed an approach for spatial modelling of spectrum usage. We have shown that semivariogram-based modelling can accurately reproduce the power spectral density (PSD) as measured at a limited number of sampling locations. We have used extensive measurement results as input for the model fitting and provided realistic parameters for multiple wireless technologies. Based on our measurement results we have also pointed out the importance of accurate sampling grid design in order to cover a large enough area without selecting a too coarse setup.

The introduced spatial spectrum model has several applications in the area of dynamic spectrum access (DSA), e.g., the evaluation of cooperative sensing techniques. Additionally, it enables the detailed analysis of emerging ideas such as online reasoning in cognitive radio networks or cooperative localization of primary transmitters [23], that later on enables a more accurate estimation of the no-talk area [24] in DSA networks. Further use in other fields of wireless communication research is also conceivable because the model is attractive due to its manageable number of parameters and the independence of the transmitter locations or the propagation characteristics. Both aspects are inherently modelled by the random field.

Our future work includes comparison of the measurement-based results to simulations. The latter approach uses a system model including, e.g., a propagation model and realistic transmitter location distributions for computation of the PSD over space. Additionally, we will extend our measurement system to four setups in order to collect further data and test other sampling grids. We also plan to make the measurement data available to the research community in appropriate format.

ACKNOWLEDGMENT

The authors would like to thank the RWTH Aachen University and the German Research Foundation (Deutsche

TABLE I
MODEL PARAMETERS FOR SELECTED WIRELESS TECHNOLOGIES.

Correlogram model	Wireless service	Measurement location	δ [dBm/100 kHz]	$\overline{\mu_{ch}}$ [dBm/100 kHz]	$\text{std}(\mu_{ch})$ [dBm/100 kHz]	Nugget τ^2	Sill σ^2	Range ϕ	κ	Quality of fit Q
Exponential	UMTS	Aachen	-	-87.83	8.0	2.0	105.27	161.14	-	19.71
Matérn	UMTS	Aachen	-	-87.83	8.0	0.0	109.73	229.58	0.34	18.47
Cauchy	UMTS	Aachen	-	-87.83	8.0	3.1	144.28	33.78	0.21	17.30
Exponential	GSM900	Aachen	-105	-82.68	6.1	17.0	98.42	191.40	-	10.10
Matérn	GSM900	Aachen	-105	-82.68	6.1	2.5	122.15	490.91	0.19	8.31
Cauchy	GSM900	Aachen	-105	-82.68	6.1	15.1	124.49	50.63	0.29	9.53
Exponential	DECT	Aachen	-105	-91.55	1.5	37.7	13.52	34.08	-	6.87
Matérn	DECT	Aachen	-105	-91.55	1.5	42.5	8.13	3.42	50.00	6.70
Cauchy	DECT	Aachen	-105	-91.55	1.5	42.4	8.23	214.54	21.54	6.72
Exponential	WLAN	Aachen	-105	-96.56	0.5	0.0	28.44	23.93	-	10.51
Matérn	WLAN	Aachen	-105	-96.56	0.5	7.9	19.24	2.05	50.00	8.45
Cauchy	WLAN	Aachen	-105	-96.56	0.5	7.9	19.24	202.72	49.89	8.45
Exponential	WLAN	CeBIT	-105	-84.59	2.1	2.4	17.46	32.38	-	16.23
Matérn	WLAN	CeBIT	-105	-84.59	2.1	0.0	20.26	39.90	0.35	16.09
Cauchy	WLAN	CeBIT	-105	-84.59	2.1	4.7	20.63	15.02	0.32	16.11

Forschungsgemeinschaft, DFG) for providing financial support through UMIC research centre. We would also like to thank the European Union for providing partial funding of this work through the ARAGORN project. Additionally, we would like to thank the Deutsche Messe AG for permitting and supporting our measurements at the CeBIT industry fair.

REFERENCES

- [1] M. A. McHenry, "NSF Spectrum Occupancy Measurements Project Summary," Shared Spectrum Company, Tech. Rep., August 2005.
- [2] M. Wellens, J. Wu, and P. Mähönen, "Evaluation of spectrum occupancy in indoor and outdoor scenario in the context of cognitive radio," in *Proc. of IEEE Second International Conference on Cognitive Radio Oriented Wireless Networks and Communications (CROWNCOM)*, Orlando, FL, USA, August 2007, pp. 420–427.
- [3] Federal Communications Commission, "Spectrum Policy Task Force," Report ET Docket no. 02-135, November 2002.
- [4] I. F. Akyildiz, W.-Y. Lee, M. C. Vuran, and S. Mohanty, "Next generation/dynamic spectrum access/cognitive radio wireless networks: a survey," *Elsevier Computer Networks Journal*, vol. 50, no. 13, pp. 2127–2159, September 2006.
- [5] Q. Zhao and B. Sadler, "A Survey of Dynamic Spectrum Access," *IEEE Signal Processing Magazine*, vol. 24, no. 3, pp. 79–89, May 2007.
- [6] A. Ghasemi and E. S. Sousa, "Collaborative Spectrum Sensing for Opportunistic Access in Fading Environments," in *Proc. of IEEE Symposium on New Frontiers in Dynamic Spectrum Access Networks (DySPAN)*, Baltimore, MD, USA, November 2005, pp. 131–136.
- [7] E. Visotsky, S. Kuffner, and R. Peterson, "On Collaborative Detection of TV Transmissions in Support of Dynamic Spectrum Sharing," in *Proc. of IEEE Symposium on New Frontiers in Dynamic Spectrum Access Networks (DySPAN)*, Baltimore, MD, USA, November 2005, pp. 338–345.
- [8] S. M. Mishra, A. Sahai, and R. W. Brodersen, "Cooperative Sensing among Cognitive Radios," in *Proc. of IEEE International Conference on Communications (ICC)*, vol. 4, Istanbul, Turkey, June 2006, pp. 1658–1663.
- [9] M. Gudmundson, "Correlation model for shadow fading in mobile radio systems," *Electronic Letters*, vol. 27, no. 23, pp. 2145–2146, 1991.
- [10] A. Jindal and K. Psounis, "Modeling spatially correlated data in sensor networks," *ACM Transactions on Sensor Networks (TOSN)*, vol. 2, no. 4, pp. 466–499, 2006.
- [11] J. Riihijärvi, P. Mähönen, M. Wellens, and M. Gordziel, "Characterization and Modelling of Spectrum for Dynamic Spectrum Access with Spatial Statistics and Random Fields," in *Proc. of 1st International Workshop on Cognitive Radios and Networks (CRNETS)*, in conjunction with *IEEE PIMRC 2008*, Cannes, France, September 2008.
- [12] N. Cressie, *Statistics for Spatial Data*, revised ed. Wiley, October 1993.
- [13] M. D. Ecker and A. E. Gelfand, "Bayesian Variogram Modeling for an Isotropic Spatial Process," *Journal of Agricultural, Biological and Environmental Statistics*, vol. 2, no. 4, pp. 347–369, 1997.
- [14] P. J. Diggle, P. J. Ribeiro, and O. F. Christensen, *Spatial statistics and computational methods*. Springer Verlag, Lecture Notes in Statistics, vol. 173, 2003, ch. An Introduction to Model-based Geostatistics.
- [15] N. Cressie, "Fitting Variogram Models by Weighted Least Squares," *Mathematical Geology*, vol. 17, no. 5, pp. 563–586, July 1985.
- [16] G. Matheron, "Principles of geostatistics," *Economic Geology*, vol. 58, no. 8, pp. 1246–1266, December 1963.
- [17] P. J. Ribeiro Jr. and P. J. Diggle, "geoR: A package for geostatistical analysis," *R News*, vol. 1, no. 2, pp. 15–18, June 2001.
- [18] M. Schlather, "Simulation of stationary and isotropic random fields," *R News*, vol. 1, no. 2, pp. 18–20, June 2001.
- [19] R Development Core Team, *R: A Language and Environment for Statistical Computing*, R Foundation for Statistical Computing, Vienna, Austria, 2007.
- [20] M. Wellens, J. Riihijärvi, M. Gordziel, and P. Mähönen, "Evaluation of Cooperative Spectrum Sensing based on Large Scale Measurements," in *Proc. of 3rd IEEE Symposium on New Frontiers in Dynamic Spectrum Access Networks (DySPAN)*, Chicago, IL, USA, October 2008.
- [21] S. Shellhammer and G. Chouinard, "Spectrum sensing requirements summary," IEEE 802.22-05/22-06-0089-05-0000, July 2006.
- [22] R. M. Lark, "Optimized spatial sampling of soil for estimation of the variogram by maximum likelihood," *Geoderma*, vol. 105, no. 1–2, pp. 49–80, January 2002.
- [23] B. L. Mark and A. O. Nasif, "Estimation of Interference-Free Transmit Power for Opportunistic Spectrum Access," in *Proc. of IEEE Wireless Communications and Networking Conference (WCNC)*, Las Vegas, NV, USA, April 2008, pp. 1679–1684.
- [24] R. Tandra, S. M. Mishra, and A. Sahai, "What is a spectrum hole and what does it take to recognize one?" *accepted for publication in Proceedings of the IEEE*, 2008.